

# Single-Cell RNA Sequencing of *Sox17*-Expressing Lineages Reveals Distinct Gene Regulatory Networks and Dynamic Developmental Trajectories

Linh T. Trinh<sup>1,2,3,4</sup>, Anna B. Osipovich<sup>1,3</sup>, Bryan Liu<sup>5</sup>, Shristi Shrestha<sup>3</sup>, Jean-Philippe Cartailier<sup>3</sup>, Christopher V.E. Wright<sup>2,3,4</sup>, Mark A. Magnuson<sup>1,2,3,4,\*</sup>

<sup>1</sup>Department of Molecular Physiology and Biophysics, Vanderbilt University, Nashville, TN, USA

<sup>2</sup>Department of Cell and Developmental Biology, Vanderbilt University, Nashville, TN, USA

<sup>3</sup>Center for Stem Cell Biology, Vanderbilt University, Nashville, TN, USA

<sup>4</sup>Program in Developmental Biology, Vanderbilt University, Nashville, TN, USA

<sup>5</sup>College of Arts and Sciences, Vanderbilt University, Nashville, TN, USA

\*Corresponding author: Mark A. Magnuson, Department of Molecular Physiology and Biophysics, Vanderbilt University, 9465 MRB-IV, 2213 Garland Avenue, Nashville, TN 37232-0494, USA. Tel: +1 615 322 7006; Fax: +1 615 322 6645; Email: [mark.magnuson@vanderbilt.edu](mailto:mark.magnuson@vanderbilt.edu)

## Abstract

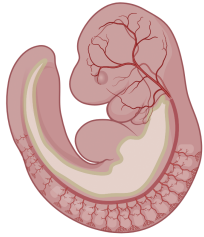
During early embryogenesis, the transcription factor SOX17 contributes to hepato-pancreato-biliary system formation and vascular-hematopoietic emergence. To better understand *Sox17* function in the developing endoderm and endothelium, we developed a dual-color temporal lineage-tracing strategy in mice combined with single-cell RNA sequencing to analyze 6934 cells from *Sox17*-expressing lineages at embryonic days 9.0–9.5. Our analyses showed 19 distinct cellular clusters combined from all 3 germ layers. Differential gene expression, trajectory and RNA-velocity analyses of endothelial cells revealed a heterogeneous population of uncommitted and specialized endothelial subtypes, including 2 hemogenic populations that arise from different origins. Similarly, analyses of posterior foregut endoderm revealed subsets of hepatic, pancreatic, and biliary progenitors with overlapping developmental potency. Calculated gene-regulatory networks predict gene regulons that are dominated by cell type-specific transcription factors unique to each lineage. Vastly different *Sox17* regulons found in endoderm versus endothelial cells support the differential interactions of SOX17 with other regulatory factors thereby enabling lineage-specific regulatory actions.

**Key words:** single-cell RNA sequencing; **Sox17**; endoderm; hepato-pancreato-biliary system; endothelium; hematopoiesis.

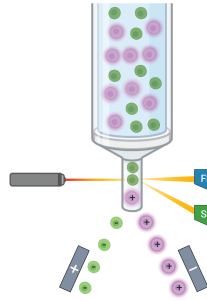
Graphical Abstract

1. Isolation of Sox17-expressing cells by dual-color FACS

*Sox17<sup>GFPcre/+</sup>;  
R26<sup>LSL.TdTomato/+</sup>*

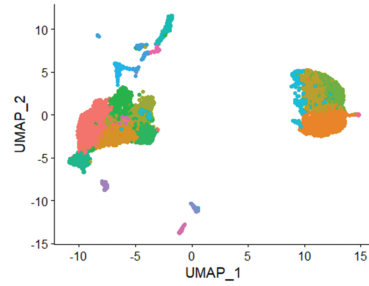


sort



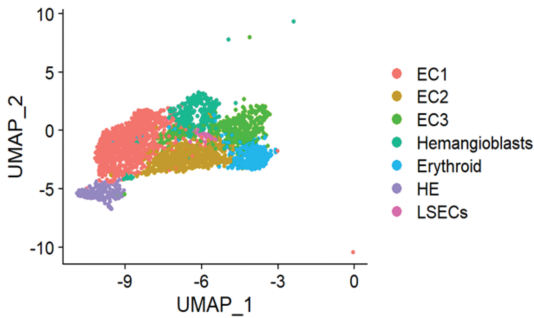
scrNaseq

Sox17-expressing lineages

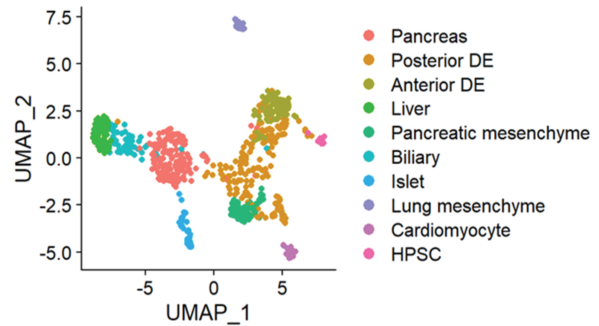


2. Transcriptomic profile and developmental trajectory analyses

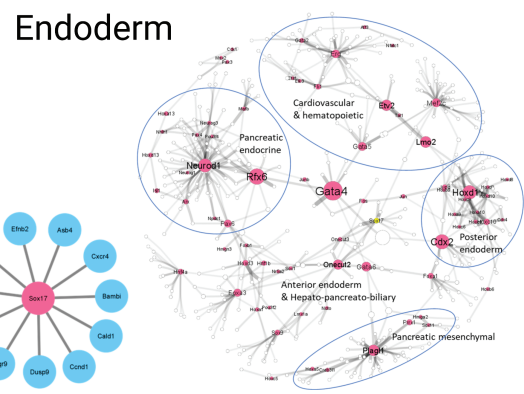
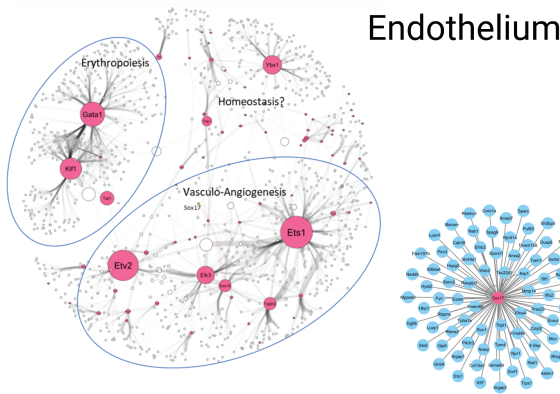
Endothelium



Endoderm



3. Identification of lineage-specific gene regulatory networks and Sox17 regulons



≠

Introduction

Sets of so-called “master” regulatory genes, such as those in the *Sry*-related SOX transcription factor (TF) family, play critical roles in a spatiotemporally modulated and hierarchically organized cascade of such networks, enabling progressively more complex specification of the many cellular lineages required for completing organogenesis. *Sox17* is a crucial contributor to multiple developmental processes

in early vertebrate embryogenesis.<sup>1-3</sup> A defining feature of all SOX proteins is a high mobility group (HMG) box domain<sup>4</sup> that binds the minor groove of the DNA double helix, resulting in DNA bending that enables the overlaying chromatin topology to be modulated.<sup>5</sup> Interactions between SOX17 and other protein partners during development enable *Sox17* to dynamically regulate target genes<sup>6-8</sup> in multiple lineages, including extra-embryonic endoderm, definitive

endoderm, vascular endothelium, hematopoietic stem cells, and oligodendrocytes.<sup>9-11</sup>

Previous analyses of bulk transcriptomic changes in *Sox17*-null embryos and *Sox17*-overexpressing cells in culture produced highly variable predictions of *Sox17* downstream targets, suggesting cell type-specific effects.<sup>12-15</sup> Single-cell RNA sequencing (scRNAseq) has enabled investigation of transcriptomic features across different cell types and developmental trajectories. While endoderm development (especially posterior foregut), and endothelium-derived hematopoiesis have been broadly subjected to scRNAseq transcriptomic analyses,<sup>16-19</sup> a more focused decoding of *Sox17* lineages is necessary to gain deeper insights into the development of subsets of endodermal and mesodermal tissues.

In this study we used a *Sox17*-centric strategy, utilizing a *Sox17*<sup>GFP<sup>Cre</sup></sup> allele alone or in combination with a *R26*<sup>LSL-TdTomato</sup> Cre reporter, to isolate *Sox17*-expressing cells from E9.0 - E9.5 embryos. scRNAseq analysis of these cells revealed multiple clusters of endoderm, endothelium, and hematopoietic cells. Trajectory analysis of the endothelial compartment identified 2 pools of hemogenic endothelial cells of different origins. By integrating the endodermal cluster with a previously published dataset,<sup>20</sup> we observed a spectrum of overlapping transcriptomic profiles among the hepatic, pancreatic, and biliary progenitors as they segregate within the posterior foregut domain. Applying pySCENIC,<sup>21</sup> which infers scRNAseq co-expression patterns between genes and further refines direct targets using existing TF binding-motif databases to predict active gene regulatory networks (GRNs) in various cell types, we identified prospective distinct endodermal and endothelial-specific gene targets for SOX17.

## Methods

### Mouse Lines

The *Sox17*<sup>GFP<sup>Cre</sup></sup> allele (*Sox17*<sup>tm1.3(CreGFP)/Mgn</sup>, MMRRC\_036463-UNC), containing a GFP<sup>Cre</sup> fusion protein in lieu of SOX17 coding sequences,<sup>22</sup> was bred into a CD1 background and maintained in a heterozygous state. Mice that are heterozygous for the *Sox17*<sup>GFP<sup>Cre</sup></sup> allele exhibit no obvious phenotype, are fertile, born at the expected Mendelian ratios, and have normal life expectancy. *Sox17*<sup>GFP<sup>Cre</sup></sup> heterozygous embryos for sequencing experiments were generated by crossing *Sox17*<sup>GFP<sup>Cre</sup></sup> heterozygous males (CD1 background) with either wild-type (CD1 background) or *R26*<sup>LSL-TdTomato</sup> (B6.Cg-Gt(ROSA)26Sor<sup>tm14(CAG-tdTomato)/Hze/J</sup>, The Jackson Laboratory, #007914) homozygous (C57BL/6J background) females. Cre-negative, *Sox17* wild-type embryos harvested from the same dam established baseline fluorescence for cell sorting. Embryos at embryonic day (E) 9.0-9.5 were dissected in cold PBS and staged by Theiler's criteria. Genotypes were from PCR analysis of yolk sac DNA and fluorescence signal (green indicating presence of *Sox17*<sup>GFP<sup>Cre</sup></sup> and red indicating recombination of *R26*<sup>LSL-TdTomato</sup> by *Sox17*<sup>GFP<sup>Cre</sup></sup>).

### Genotyping

Tail or yolk-sac tissue digested with proteinase K was analyzed by PCR assay detecting wild-type or mutant *Sox17* allele with EconoTaq PLUS 2X Master Mix (Biosearch Technologies, #30035). Primers (forward: 5' CAGAGGTATGCAGATCTCTGT 3' and reverse: 5' CATTCTGGTCAACATGTAAGGT 3') were annealed at 57°C.

## Fluorescence-Activated Cell Sorting

Embryos were incubated for 10 min at 37 °C with Accumax (Millipore Sigma, #A7089) supplemented with DNase (Life Technologies, #AM2222; 1:1000 dilution ratio), and further disaggregated by vigorous pipetting during incubation. Passing the cell suspension through 35 µm strainer caps (Corning, #352235) led to single cells, which were washed with FACS buffer (R&D systems, #FC001) and pelleted at 4 °C, 1000 rpm for 3 min. Cells were resuspended in FACS buffer containing DNaseI (1:1000 dilution) and stained with 7AAD (15 min, room temperature—RT). Live cells (7AAD-negative) expressing either GFP or TdTomato fluorescence were then sorted into DMEM with 10% FBS at the Vanderbilt Flow Cytometry Shared Resource.

## Sequencing and Computational Analysis

Cell suspensions were processed for 3'-scRNAseq by the 10X Chromium system. A NovaSeq 6000 device was used to acquire 150 bp paired-end reads. Base calling was performed by RTA (version 2.4.11; Illumina), and further analysis was carried out using 10X Genomics Cell Ranger software v3.0.2. Initial quality control filtration, unsupervised clustering, and differential gene expression analysis used Seurat 4.<sup>23</sup> Doublet prediction used DoubletFinder.<sup>24</sup> Pseudotime analysis used Monocle 3,<sup>25</sup> while RNA velocities were calculated with scVelo.<sup>26</sup> pySCENIC<sup>21</sup> was used to infer gene regulatory networks with downstream visuals by Cytoscape<sup>27</sup> and ComplexHeatmap.<sup>28</sup>

## Data Availability

Raw scRNAseq data is at ArrayExpress (E-MTAB-12719), Seurat objects are at [https://zenodo.org/record/7725887#.ZA5jRR\\_MLkI](https://zenodo.org/record/7725887#.ZA5jRR_MLkI), and scripts used to perform quality control, clustering, differential gene expression analysis, Monocle3 and RNAvelocity analyses are at <https://github.com/markmagnuson/2023-Linh-scRNASeq-Mouse-Sox17-Expressing-Lineages>.

## Immunofluorescence Staining

Embryos were fixed with 2% PFA (1 h, RT), incubated in 30% sucrose (overnight, 4 °C), embedded in OCT (Sakura, #4583). Eight micrometre-thick embryonic sections were post-fixed with ice-cold acetone (30 min, RT), permeabilized with 0.3% Triton X-100 (10 min, RT), and blocked with 3% BSA (1 h, RT). Primary antibodies (Supplementary Table S1) were diluted in 1% BSA for staining (overnight, 4 °C). After 3 PBST (0.2% Tween in PBS) washes, secondary antibodies (Supplementary Table S1) were incubated (1 h, RT), followed by 3 PBST washes and autofluorescence quenching with Vector TrueVIEW (following manufacturer protocol; Vector Laboratories, #SP-8400-15). Stained sections were mounted with Vectashield (Vector Laboratories, #H-1700) and imaged using Zeiss LSM710 confocal microscope.

## Results

### *Sox17*<sup>GFP<sup>Cre</sup></sup> Expression Faithfully Reflects Known *Sox17*-Expressing Lineages and Suggests Several New *Sox17*-Expressing Cell Types

To better define *Sox17* gene expression at E9.5, a dynamic time during gastrulation when multiple *Sox17*-associated cellular diversifications are occurring, we began

with immunofluorescence labeling of SOX17, PECAM1, and FOXA2, marking previously known *Sox17*-expressing lineages (Fig. 1A). As expected, SOX17 was detected mainly in PECAM1<sup>+</sup> vascular cells and FOXA2<sup>+</sup> endoderm. Nuclear signals were also present in scattered SOX17<sup>+</sup> cells not producing either PECAM1 or FOXA2, located mostly along the dorsal side of embryos (Fig. 1B), suggesting previously unreported *Sox17*-expressing lineages or sites of aberrant gene expression.

To characterize *Sox17*-expressing populations we developed a dual-color lineage-tracing strategy by intercrossing *Sox17<sup>GFP</sup>Cre<sup>+</sup>* (Fig. 1C) and *R26<sup>LSL.TdTomato</sup>* Cre-reporter mice, to enable identification of short and long-term progeny of *Sox17*-expressing lineages based on GFP and TdTomato production. Immuno-labeling of SOX17, GFP, and TdTomato in E9.5 embryonic sections confirmed SOX17 colocalization with all GFP, while most TdTomato-positive cells did not have GFP or SOX17 (Fig. 1D), indicating short-term longevity of the GFP-Cre fusion protein and robustness of the dual-color tracing strategy. While TdTomato intensity was uniform throughout the embryos, GFP fluorescence varied within the emerging endoderm at E8.5-E9.5 reflecting temporally varying *Sox17* expression throughout the foregut, midgut, and hindgut (Supplementary Fig. S1). Within mesodermal tissues, TdTomato but not GFP was present mostly in the heart at E8.5-9.0, while a mixture of both fluorescence signals was observed within the vasculature in other embryonic regions by E9.5 (Supplementary Fig. S1).

## Single-Cell Transcriptomic Analysis Reveals Canonical and Non-Canonical *Sox17*-Expressing Cells

Two separate E9.0-9.5 single-cell collections were prepared from our dual-color strategy (Fig. 2A) using *Sox17<sup>GFP</sup>Cre<sup>+</sup>* males mated with wild type or *R26<sup>LSL.TdTomato</sup>/LSL.TdTomato* females. The first sample reporting *Sox17* short-term expression was prepared on the basis of GFP produced from a mixture of *Sox17<sup>GFP</sup>Cre<sup>+</sup>*; *R26<sup>+/+</sup>* and *Sox17<sup>+/+</sup>*; *R26<sup>+/+</sup>* embryos. The second sample was isolated from *Sox17<sup>GFP</sup>Cre<sup>+</sup>*; *R26<sup>LSL.TdTomato</sup>+/+* embryos were identified by red fluorescence, and comprised cells derived over a short period after *Sox17* expression indicated from their green/red co-fluorescence, or over a longer period by being only red. scRNAseq produced 2 datasets, hereafter referred to as GFP and TdTomato datasets, which were analyzed separately to filter out low-quality cells and predicted doublets (Supplementary Figs. S2 and S3). The integrated (GFP and TdTomato) dataset contained 6934 cells segregated into 19 clusters (Fig. 2B) belonging to 3 main lineages: endoderm (*Epcam*<sup>+</sup>), endothelium (*Pecam1*<sup>+</sup>), and hematopoietic cells (*Hba-a1*<sup>+</sup>) (Supplementary Fig. S3).

Cell identities were assigned via differential expression analysis (Fig. 2C). The endothelial lineage (*Cd31/Pecam1*<sup>+</sup>, *Tie2/Tek*<sup>+</sup>) consisted of hemangioblasts (*Etv2*<sup>+</sup>, *Tal1*<sup>+</sup>), 3 different clusters of endothelial cells (EC1 to EC3) (differing by expression of histone H1 genes, extracellular matrix *Vwa1*, and *Hox* genes), endocardium (*Hand2*<sup>+</sup>), liver sinusoidal endothelial cells (LSEC—*Oit3*<sup>+</sup>, *Stab2*<sup>+</sup>), and hemogenic endothelium (HE—*Cd44*<sup>+</sup>, *Sox17*<sup>+</sup>). The next most abundant

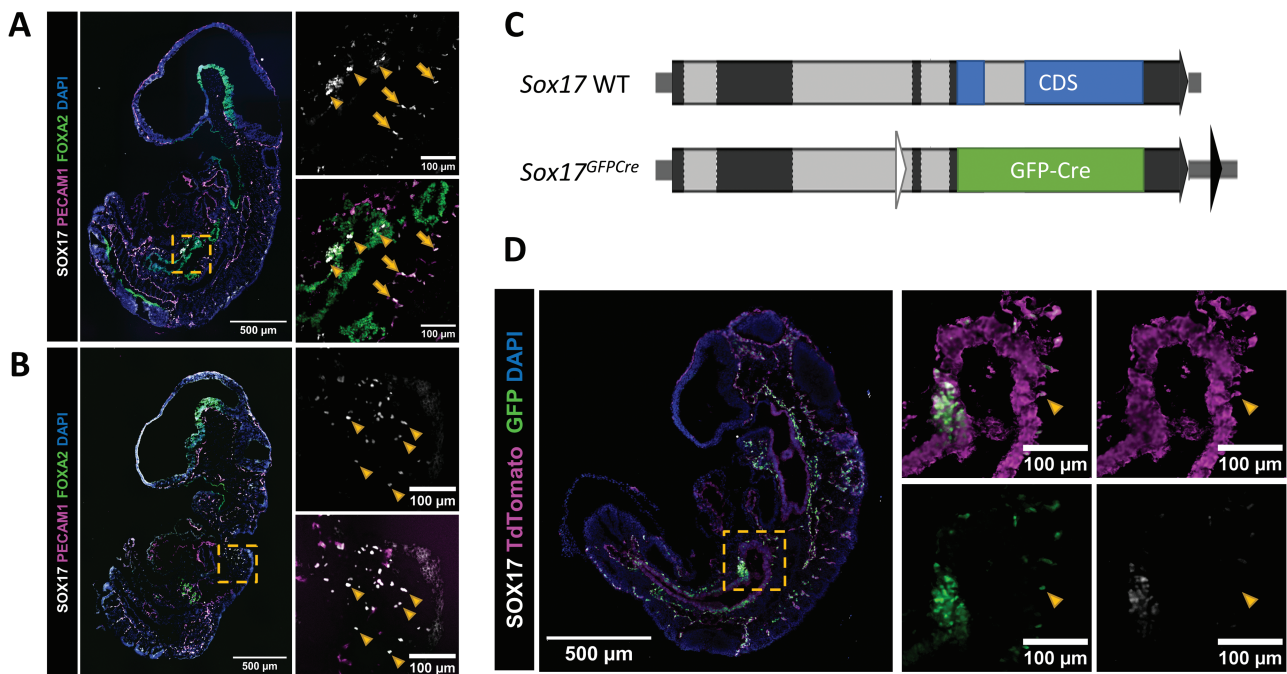


**Figure 1.** Temporal lineage tracing of *Sox17* expression with a dual color system in mice. (A) Representative image and inset of immunofluorescence labelling of an E9.5 mouse embryonic section showing nuclear SOX17 staining (colocalizes with DAPI staining) seen in both endodermal cells (positive for FOXA2—arrowheads) and endothelial cells (positive for PECAM1—arrows). (B) Representative image and inset of immunofluorescence labelling of an E9.5 mouse embryonic section showing SOX17 positive cells that are not positive for either FOXA2 or PECAM1 staining, arrowheads. (C) *Sox17* temporal lineage tracing allele with full-length SOX17 protein coding sequence (CDS) replaced with a sequence coding for GFP-Cre fusion protein (black boxes—exon; gray boxes—intron; blue and green boxes—protein coding sequences; black and white triangles—retained loxP sites after recombinase-mediated cassette exchange strategy used to generate the allele.<sup>22</sup> (D) Immunofluorescence labelling of SOX17, GFP, and TdTomato in *Sox17<sup>GFP</sup>Cre<sup>+</sup>*; *R26<sup>LSL.TdTomato</sup>+/+* E9.5 embryonic sections. Inset shows a group TdTomato positive cells with the majority are negative for both GFP and SOX17 and a small portion positive for GFP but not SOX17, as indicated by arrowhead.

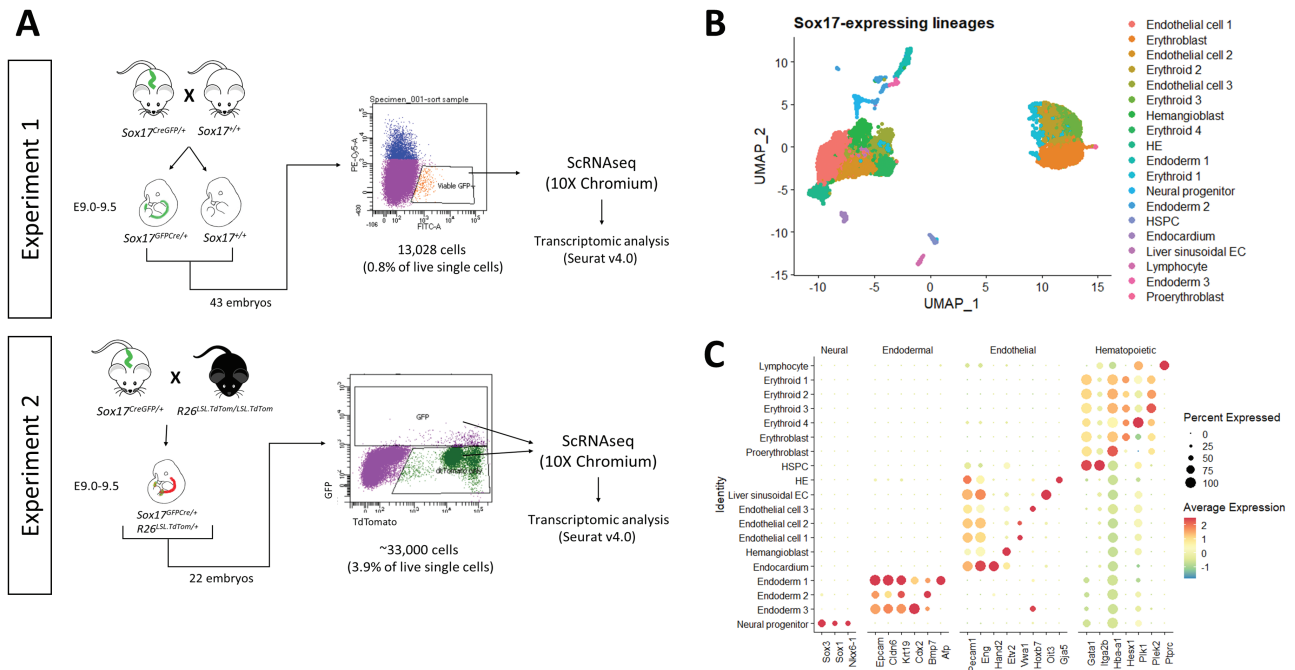


**Figure 2.** Single-cell RNA sequencing of murine *Sox17*-expressing lineages using the temporal dual color tracing system captured both expected and non-canonical *Sox17*-expressing cell types. **(A)** Experimental layout of 2 scRNAseq experiments. At around E9.5, single cells from embryos with desired genotypes are isolated for subsequent flow cytometry sorting and RNA sequencing with 10X Chromium platform. Datasets were analyzed using Seurat package version 4.0. **(B)** UMAP visualization of the integrated *Sox17*-expressing lineage dataset. Cells were colored based on clusters identified by unsupervised clustering. Cell types were defined based on differential gene expression analysis. **(C)** Expression of representative marker genes for each cell cluster. *Epcam*, *Cldn6*, and *Krt19* served as shared markers for 3 endodermal clusters; *Pecam1* and *Eng* for 7 endothelial clusters; and *Gata1*, *Itga2b*, and *Hba-1* for 8 hematopoietic clusters. The rest of the genes are differentially expressed by individual clusters ( $P$ -adjusted < .05). Dot color and size indicate gene expression intensity and percentage of cell expressing genes of interest, respectively.

cell group represented hematopoietic lineages, with 4 distinct erythroid clusters, one of which lies proximate to the endothelial island. Three endodermal clusters were identified with scattered expression of hepatic (*Afp*), pancreatic (*Pdx1*), anterior endoderm (*Sox2*), and posterior endoderm (*Cdx2*) markers. A small number of neuronal progenitors (*SoxB*<sup>+</sup>, *Nkx6.1*<sup>+</sup>) were *Sox17*<sup>-</sup>, suggesting putative emergence from *Sox17*-expressing progenitors. Together, the 2 datasets reflected known *Sox17* expression patterns in endodermal, endothelial, and hematopoietic cells, and also suggested *Sox17* expression in rare neuronal-lineage cells.

### scRNAseq of *Sox17*-Expressing Endothelium Captures Transcriptional Signatures of Early Vasculogenesis, Angiogenesis, and Erythropoiesis

Based on *Cd31/Pecam1* expression and tight clustering, the endothelial compartment was defined as EC1/2/3, hemangioblast, HE, erythroid 1, and LSEC (Fig. 3A, 3B). Since there were 3 distinct clusters of ECs that did not differentially express any endothelial subtype (arterial/venous/capillary/lymphatic) markers, we distinguished them based on their transcriptional profiles. EC3 expressed relatively high levels of *Hox* genes, also a feature of the HE cluster, which is known for regulating hematopoiesis<sup>29</sup> (Supplementary Fig. S4A), suggesting hematopoietic potential. Of note, although the yolk sac was specifically omitted from our dissections, a small portion of EC3 expressed signature placental genes *Plac1* and *Nrk*<sup>30,31</sup> (Supplementary Fig. S4B), suggesting an extraembryonic (perhaps mobile) origin of EC3. EC1 and EC2 differed mostly by cell-cycle gene expression (Supplementary Fig. S4D). EC1 expressed significantly higher levels ( $P$ -adjusted

< .05) of *Cdc20*, *Cenpa*, *Ccnb2*, and *Tuba1c*, suggesting mitotic status, whereas EC2 had higher expression of *histone H1*, *Top2a*, *Cdk1*, and *Aurkb* more fitting the G2-like state.<sup>32</sup> However, Seurat cell-cycle scoring predicts a large portion of EC2 cells are in S phase whereas those in the EC1 cluster are in either the G1, G2/M, or S phases (Supplementary Fig. S4C).

Observing progenitor-type and further-differentiated endothelial cells both near a cluster of erythroid cells suggested that *Sox17*-lineages include cells progressing through vasculogenesis and endothelium-derived hematopoiesis. To assess the transcriptomic alterations of such cells occurring within these individual processes, we performed Monocle 3 trajectory analysis to order cells in pseudotime<sup>33</sup> and used scVelo RNA velocity to reveal putative transitional directions between cells<sup>26,34</sup> (Fig. 3C). While scVelo uses the unbiased RNA spliced/unspliced ratio, Monocle 3 requires supervised input of the trajectory root, which we selected based on *Etv2* defining the conventional hemangioblast population. These analyses recapitulated a well-established model whereby hemangioblasts give rise either indirectly to hemogenic endothelium through the differentiation of EC1 cells (pathway a), or directly to the non-hemogenic EC2 cells (pathway b) (Fig. 3D). In addition, they revealed a potentially bipotent progenitor group EC3, which may originate from mobile yolk-sac cells that become either EC2 (pathway c) or erythroid cells (pathway d).

Because HE and EC3 clusters both express multiple *Hox* genes known to drive hematopoiesis, we further resolved the transcriptional distinctions between these 2 populations. Differential expression analysis ( $P$ -adjusted < .05) revealed arterial-related signatures for HE that include

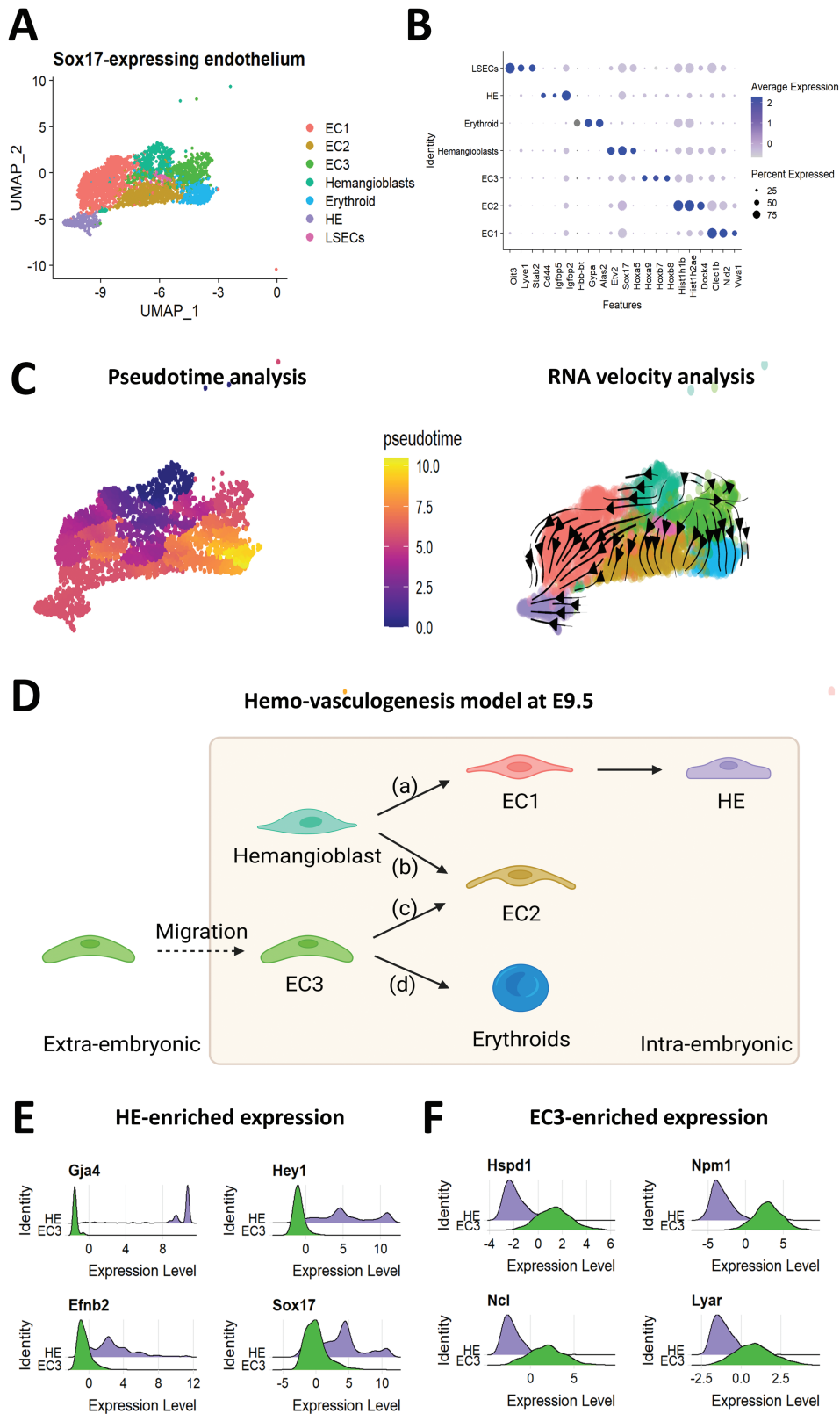


**Figure 3.** Heterogenous continuum of endothelial cell states during vasculogenesis and endothelium-derived hematopoiesis. **(A)** UMAP visualization of the *Sox17*-expressing endothelium subset colored by initial unsupervised clustering of the *Sox17*-expressing dataset. **(B)** Transcriptional level of top 3 differentially expressed genes by each cluster. Dot color and size indicate gene expression intensity and percentage of cell expressing genes of interest, respectively. **(C)** Developmental trajectory analysis of the *Sox17*-expressing endothelium subset. Pseudotime assignment was performed using Monocle3. RNA velocity streamlines were generated with scVelo and then overlaid with UMAP embeddings colored by cell types in (A). **(D)** Proposed model of multiple developmental pathways from distinct origins to specified endothelial subtypes. Hemangioblasts can give rise to hemogenic endothelial cells (HE) via endothelial cell 1 (EC1)—pathway (a), or directly to EC2—pathway (b). EC3 can differentiate to either EC2—pathway (c) or directly to erythroid cells—pathway (d). Liver sinusoidal endothelial cells (LSEC) appear to be in pathway (c). **(E)** Expression of arterial marker genes in HE and EC3. **(F)** Expression of hemogenic marker genes in HE and EC3.

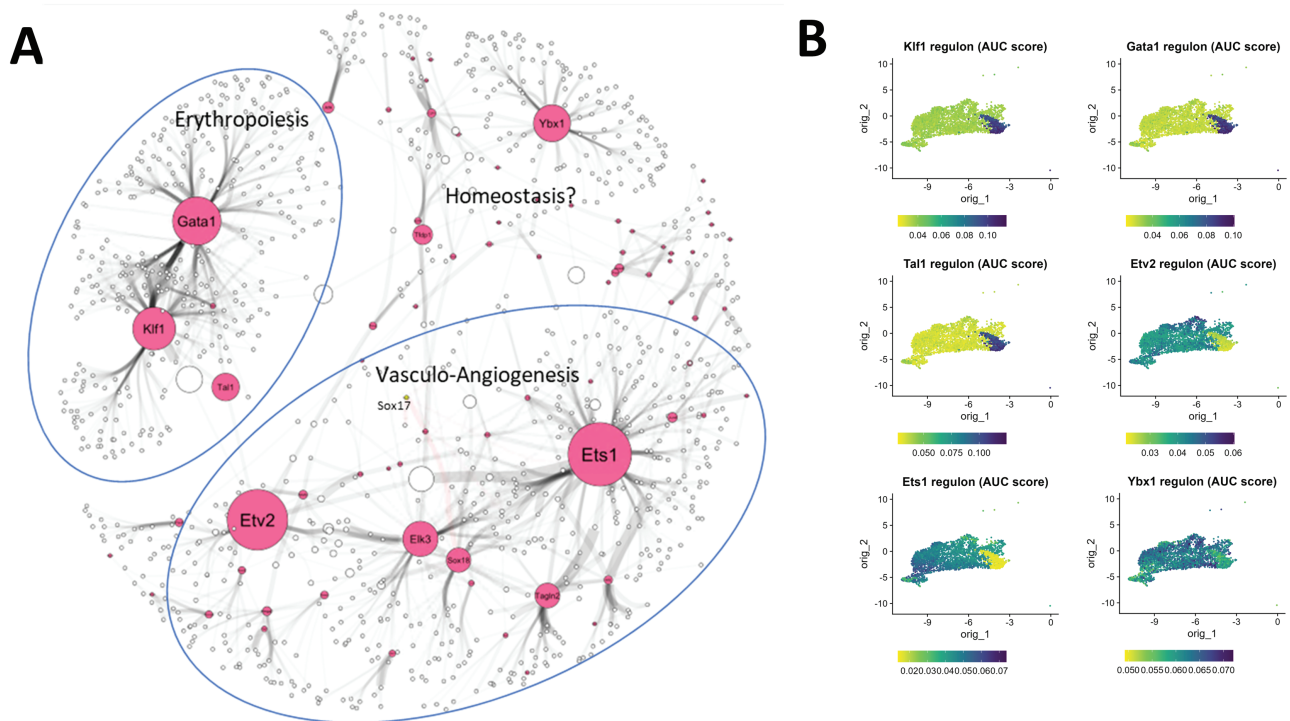


**Figure 4.** Predicted active regulons in the endothelium. **(A)** Network plot of top 10% predicted regulons ranked by “importance” metric (signifying strength of TF-target gene relation). TF (pink nodes) and connected to target genes (white nodes) via edges (gray). *Sox17* node is highlighted in yellow. Thicker to thinner edges indicate stronger to weaker relation of TF-target respectively. The size of each node represents the “betweenness centrality” measurements (possible measure of “hub” gene due to high TF-targets connectivity) of a given TF within the network. Regulon networks are manually classified into bigger gene modules (blue circles) based on known biological functions of master regulator genes. **(B)** Single-cell AUC scores (area under the recovery curve across genes ranked by expression value indicating the enrichment of each regulon in each cell) measure for 6 most prominent regulons embedded on UMAP.

gap-junction genes (*Gja4*, *Gja5*) that become upregulated by Notch signaling (marked by *Hey1*) under shear stress.<sup>35</sup> Consistent with *Sox17*-expression itself being a marker for arterial specification,<sup>36</sup> HE cells also express *Ephrin B2*, a classical arterial marker<sup>37</sup> (Fig. 3E). On the other hand, EC3 express *Hspd1* (heat-shock gene involved in yolk-sac erythropoiesis<sup>38</sup>), *Npm1* (important modulator of primitive hematopoiesis<sup>39</sup>), *Ncl* (promoter of the hemogenic GRN<sup>40</sup>), and *Lyar* (necessary for hemocyte generation<sup>41</sup>) (Fig. 3F), suggesting the extraembryonic origin and strong hemogenic potential of EC3. Together, these data are consistent with contribution of extra-embryonic ECs to intra-embryonic blood-vessel formation and suggest the existence of at least 2 EC populations with hemogenic potency from different origins at E9.5.

### Distinct Hematopoietic, Vasculo-Angiogenic, and Homeostatic Regulons in the Endothelial Lineage

Given that scRNAseq of *Sox17*-expressing lineages unbiasedly captured the dynamic transcriptional changes of vascular formation and endothelial-to-hematopoietic transition of cells from extra- and intra-embryonic sources, we attempted to unveil the key GRNs underlying these important developmental processes. By performing pySCENIC regulon analysis to infer groups of active genes that are regulated as units, with putative direct regulation defined by TF binding motifs located within likely *cis*-regulatory regions of target genes,<sup>21</sup> we identified 287 regulons among the endothelial compartment clusters. Plotting the top 10% of such regulons revealed 3 distinct GRN clusters for erythropoiesis, vasculo-angiogenesis, and

potential homeostasis of endothelial cells (Fig. 4A). Regulons of the well-established *Klf1/Gata1/Tal1* triplet—master regulators of hematopoiesis<sup>42,43</sup>—clustered tightly together (Fig. 4A) and are active specifically in erythroid 1 cluster (Fig. 4B), validating the reliability of pySCENIC predictions.

The 2 biggest nodes in the GRN are *Etv2* and *Ets1*, known pioneer TFs during embryonic vasculo-angiogenesis.<sup>44,45</sup> Although *Ets1* may have redundant functions with *Etv2* (from studies in zebrafish<sup>46</sup>), not many shared targets are observed by our regulon prediction, suggesting cross-species variation. Regulons of *Elk3* and *Sox18*, which contribute to lymphatic vascular development,<sup>47,48</sup> are clustered closely and overlap with parts of the *Etv2* and *Ets1* regulons, consistent with *Elk3* and *Sox18* regulating a more focused lymphatic subset of endothelial differentiation. Of note, *Elk3* may antagonize *Ets1* transcriptional activation to suppress angiogenesis,<sup>49</sup> likely through shared targets of *Elk3* and *Ets1*. *Tagln2*, a marker of smooth-muscle cells recently documented for its function during angiogenesis,<sup>50</sup> also forms a large node in the endothelial GRN.

Somewhat distinct from the erythropoietic and vasculo-angiogenic GRNs are the regulons for *Ybx1* and *Tfdp1* (Fig. 4A), general TFs that regulate proliferation, apoptosis, and differentiation in a non-cell-type-specific manner, often being linked to cancer progression.<sup>51-54</sup> Some angiogenic-specific functions such as proliferation, apoptosis, migration, and tubulogenesis are associated with *Ybx1*<sup>51,55,56</sup> but its regulon is notably different from other angiogenic regulons. Its activity in both endothelial and erythroid cells (Fig. 4B) suggests a more general cellular homeostatic function.

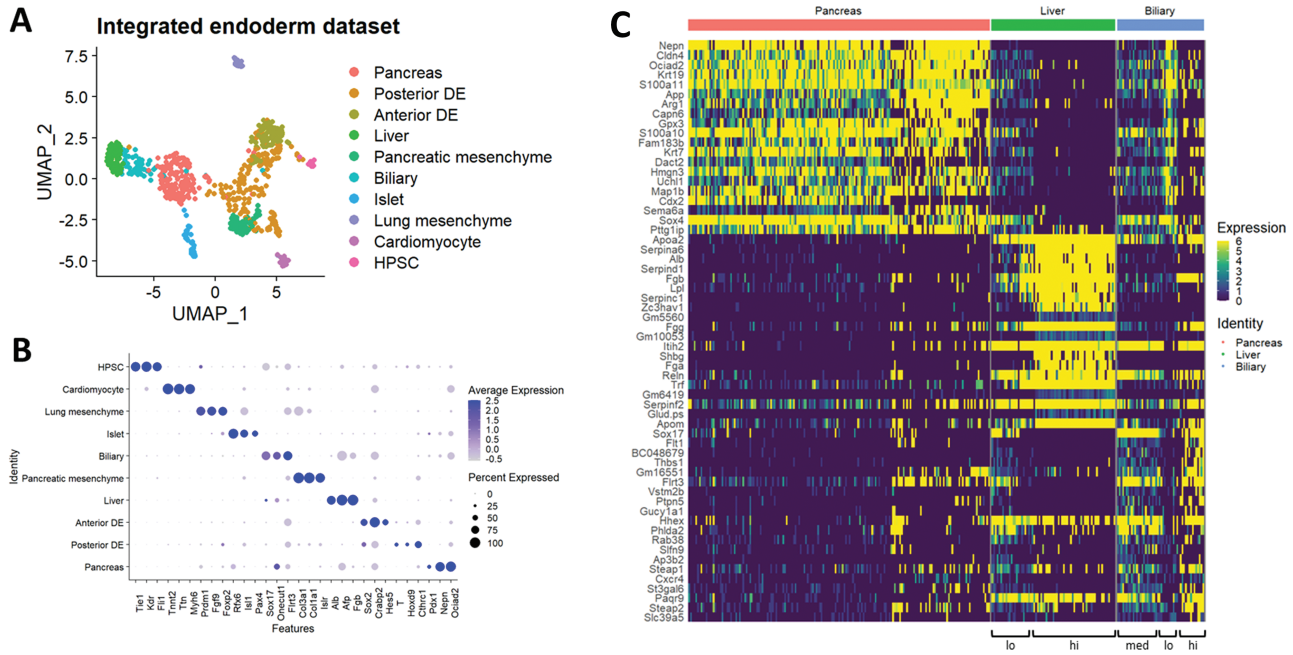


**Figure 5.** Dynamic expression profiles of hepato-pancreato-biliary cells during foregut endoderm organogenesis. **(A)** UMAP visualization of the integrated endodermal subset. Cells were colored based on clusters identified by unsupervised clustering. Cell types were defined based on differential gene expression analysis. **(B)** Transcriptional level of top 3 marker genes defining cell type of each cluster. Dot color and size indicate gene expression intensity and percentage of cell expressing genes of interest, respectively. **(C)** Heatmap of top 20 differentially expressed genes by distinct groups of progenitor cells within the developing hepato-pancreato-biliary system. Hepatic and biliary progenitor clusters are further divided into subgroups based on the expression level of organ-specific genes (lo—low; med—medium; hi—high).

Unsupervised clustering of endothelial PySCENIC regulons revealed a cluster specifically activated in hemogenic endothelium (Supplementary Fig. S5) that contains genes previously linked to the emergence of hematopoietic stem cells, such as *Runx1*, *Hox* genes, *Bcl11a*<sup>57,58</sup> and the more recently investigated *Gata3*, *Cdx4*, *Cdx1*, and *Gli3*.<sup>59-61</sup> Although *Sox17*, required for endothelial-to-hematopoietic transition,<sup>62</sup> was not found in this cluster, 4 other *Sox* members were: *Sox7* (interacts with *Runx1* to specify HE in the yolk sac<sup>63</sup>), *Sox6* (suppresses embryonic globin genes during definitive erythropoiesis<sup>64</sup>), and *Sox2* and *Sox21* (unknown functions in vascular and hematopoietic lineages). *Foxf1*, which is important for endothelial progenitors and vessel sprouting,<sup>65</sup> and *Foxn3*, which is detected in human hemogenic endothelium but has unknown function,<sup>66</sup> also appear in this HE-specific regulon cluster, suggesting previously unknown functions of these genes during endothelium-derived hematopoiesis.

### New Insights Into Hepato-Pancreato-Biliary Development by scRNAseq Analysis of *Sox17*- and *Prox1*-Expressing Endodermal Lineage

Toward better understanding endodermal, and especially hepato-pancreato-biliary (HPB) development, we re-clustered 392 endodermal cells identified in both the GFP and TdTomato datasets (“*Sox17* endoderm dataset”) to identify early progenitor cells of various organs (Supplementary Fig. S6A, S6B). Within this dataset, pancreatic progenitors (*Pdx1*<sup>+</sup> and *Rfx6*<sup>+</sup>), and hepatobiliary progenitors (*Sox17*<sup>+</sup>, *Hbex*<sup>+</sup>, and *Prox1*<sup>+</sup>) were most abundant. Since HPB cell numbers were insufficient to resolve the transcriptional segregation of progenitor cells from the 3 independent organ anlagen we combined our *Sox17* endodermal dataset with a dataset recently reported from the Spagnoli group obtained via sorting

*Prox1*-expressing cells,<sup>20</sup> hereafter called the “*Prox1* dataset.” The *Prox1* dataset contains 346 posterior-foregut cells from embryos at multiple stages during mid-gestation. Analysis of 738 cells combined from the *Sox17* endoderm (392 cells) and *Prox1* (346 cells) datasets, hereafter the “*Sox17-Prox1* endoderm” dataset, resulted in 10 distinct clusters consisting mostly of endoderm and a few mesoderm-derived cell types such as cardiomyocytes, HPSCs, pancreatic and lung mesenchyme (Fig. 5A). There was high integration across the original *Sox17* endoderm and *Prox1* datasets (Supplementary Fig. S6C; Supplementary Table S2). Cell-type assignments of the *Sox17-Prox1* endoderm dataset based on differentially expressed genes (Fig. 5B) were mostly consistent with the previous manual-dissection-based assignments of the *Prox1* dataset (Supplementary Fig. S6D; Supplementary Table S2).

After obtaining 3 distinct clusters of HBP progenitors, we performed differential transcriptomic analysis during their segregation to identify new markers for each progenitor population. We not only identified 287 significantly upregulated genes for pancreatic buds, 624 for liver bud, and 23 for biliary (*P* adjusted < .05) (top 20 differentially expressed genes are listed in Fig. 5C), but also observed substantially overlapping transcriptional profiles among the HBP progenitors.

Pancreatic markers included: *Nepn* (expressed in the dorsal pancreatic bud and duodenum by E9.5<sup>67</sup>), *Cldn4*, *Krt7*, and *Krt19* (epithelial markers highly expressed in pancreatic but absent from hepatic bud<sup>68</sup>), *Ociad2* (unknown function in embryonic pancreatic development but consistent with previous observations<sup>69</sup>), *App*, *S100a10*, and *S100a11* (involved in pancreatic cancer and diseases, patterns not yet reported during embryonic development<sup>70,71</sup>), *Cdx2* (marking caudal gut tube), and *Sox4* (expressed in pancreatic buds and important for endocrine-cell development<sup>72</sup>). Other genes identified



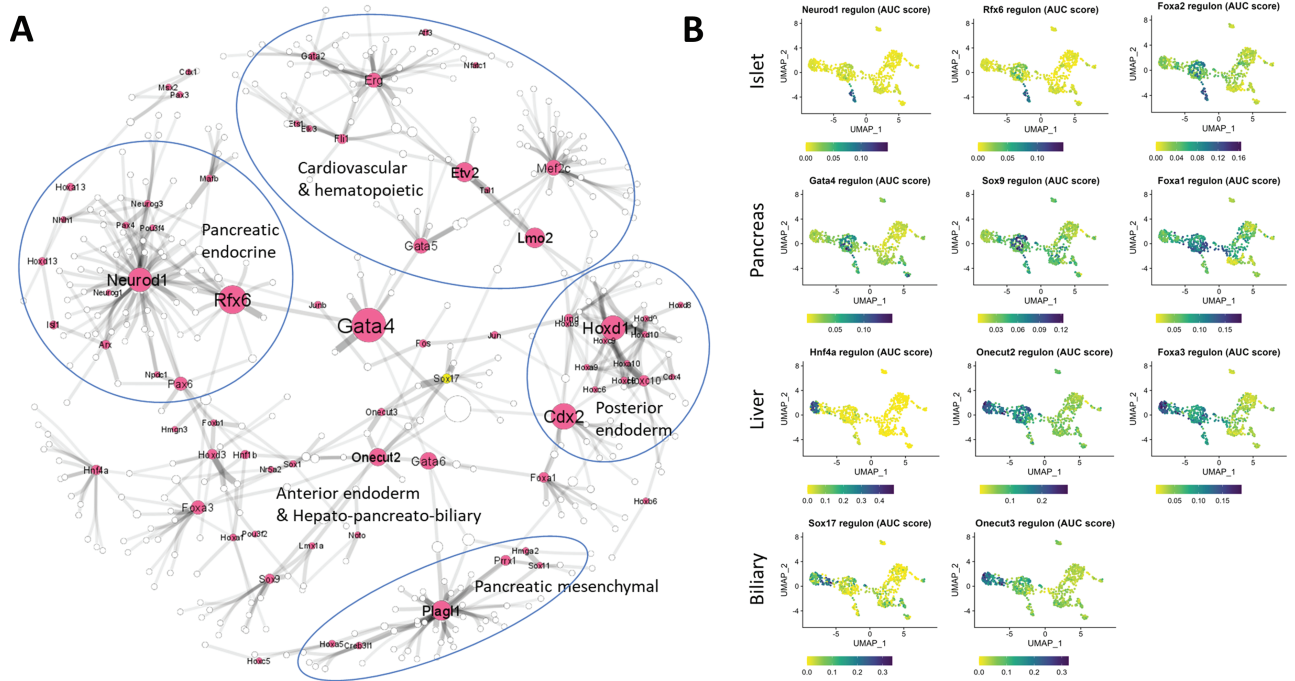


**Figure 6.** Predicted active regulons in the endoderm. **(A)** Network plot of top 10% predicted regulons ranked by “importance” metric signifying strength of TF-target relation. TF (pink nodes) and connected to target genes (white nodes) via edges (gray). *Sox17* node is highlighted in yellow. Thicker to thinner edges indicate stronger to weaker relation of TF-target respectively. The size of each node represents the “betweenness centrality” measurements (possible measure of “hub” gene due to high TF-targets connectivity) of a given TF within the network. Regulon networks are manually classified into bigger gene modules (blue circles) based on known biological functions of master regulator genes. **(B)** Single-cell AUC scores (area under the recovery curve across genes ranked by expression value indicating the enrichment of each regulon in each cell) measure for 8 most prominent regulons embedded on UMAP.

as hepatic markers were previously described as highly expressed in liver buds such as *Apo*, *Serpin*, and *Fibrinogen* gene families, *Alb*, *Reln*,<sup>73,74</sup> and those active in mature liver cells such as *Itih2*, *Shbg*, *Lpl*, and *Trf*.<sup>75-78</sup> *Sox17*, the most established marker of the biliary bud,<sup>79</sup> was also the most highly upregulated gene in biliary progenitors. *Flrt3*, reported in the original manuscript of the *Prox1* dataset,<sup>20</sup> exhibited similar expression to *Sox17*, and may be a new marker of biliary progenitors. *Itih2*, *Reln*, *Hhex*, and *Paqr9* shared the pattern of *Sox17* expression in biliary progenitors but were also upregulated in the liver, suggesting shared characteristics between biliary and hepatic progenitor cells.

Other top biliary-specific genes exhibited high, medium, or low expression, subdividing the biliary cluster into 3 groups (Fig. 5C, *P*-adjusted < .05). The biliary-low group had a high level of pancreatic markers, suggesting that they were not yet developmentally resolved but more akin to the ventral pancreatic state. The biliary-high group was likely more mature biliary epithelial cells whereas the biliary-medium group showed medium levels of pancreatic genes, indicating putative pancreato-biliary bipotent progenitor status. A similar group of biliary-medium/pancreatic-medium genes was found in part of the hepatic cluster carrying low levels of liver markers. These findings are consistent with the existence of multi- and bi-potent pools of progenitor cells during progressive segregation of the 3 foregut anlagen that is under way at E9.0-9.5. Besides having high *Sox17* expression, these putative multi- and bipotent progenitors expressed *Phlda2*, previously verified as expressed in ventral definitive endoderm<sup>80</sup> yet without a known function in early endodermal organogenesis.

### Active Regulons During Endodermal Development

To identify putative GRNs governing HBP segregation from the posterior foregut, specifically not yet addressed in the literature, we performed pySCENIC analysis on the *Sox17-Prox1* endoderm dataset, which identified 238 regulons. The top decile was shown in the network plot (Fig. 6A) with further clustering of regulons corresponding to specific cell types based on node proximity and cell types in which regulons were imputed as most active (Fig. 6B).

Besides regulons specific to non-endodermal cell types such as cardiovascular-hematopoietic lineages and pancreatic mesenchyme, we classified 3 separate regulon hubs related to the development of the early endoderm and HBP system. We inferred a dense cluster of medial and caudal *Hox* regulons that, together with *Cdx2* and *Cdx4* regulons, are predicted in posterior endoderm. Besides a role for *Cdx2* in establishing the caudal part of the gut-tube axis, genes in its regulon are more active in pancreatic buds than in liver, biliary, or islet cells, suggesting additional contribution to early pancreas formation.

Another distinct pancreatic endocrine-centric regulon cluster had major nodes of *Neurod1* and *Rfx6*, connected with *Neurog3*, *Neurog1*, *Isl1*, *Mafb*, *Pax6*, *Pou3f4*, *Arx*, and *Pax4*, all encoding TFs involved in islet endocrine-cell differentiation programs.<sup>81,82</sup> *Nhlh1* and *Npdc1* regulons were specific to the islet cluster, but as of now, lack identified functions here.

The rest of the network was classified as anterior endoderm and HBP-focused regulon hubs. *Gata4*, *Sox9*, *Foxa1*, *Hnf1b*, *Gata6*, *Jun*, and *Fos* regulons are inferred as strongly active in pancreatic progenitor cells. *Hnf4a*, *Foxa3*, and

*Nr5a2*, which shared some target genes, were upregulated in hepatic progenitors, suggesting their coordinate regulation of hepatic-bud formation and outgrowth.<sup>83,84</sup> While the *Onecut2* regulon was equally active among the 3 HPB domains, the *Onecut3* regulon was restricted to hepato-biliary progenitors. *Sox17* was the only biliary-major regulon in the mapped network. *Sox1*, *Foxb1*, *Hoxd3*, *Hoxa1*, and *Pou3f2* regulons were identified specifically in the anterior DE population. Of note, regulons associated with the same cell type were not clustered tightly together, reflecting their few shared targets, and implying diverse molecular functions for each regulon responsible during the development of each individual organ. In contrast, the mingling together of regulons important for pancreas, liver, biliary, and anterior endoderm suggests shared target genes among these cell types, in keeping with their overlapping transcriptomic profiles.

### Distinct *Sox17*-Regulons Between Endoderm and Endothelium

Perhaps the most important part of this study is our identification of highly independent regulons for *Sox17* in endoderm versus endothelium. While pySCENIC predicts 81 endothelial targets for *Sox17*, only 11 were endoderm-selective (Fig. 7A). To partially validate these targets, we surveyed 3 recently published SOX17 ChIP-seq and CUT&RUN datasets from cell-line-derived human definitive endoderm and mouse primitive endoderm and found the majority of pySCENIC-predicted endodermal targets also exhibit SOX17 binding within promoter-proximal regions (Supplementary Fig. S7). Among these genes regulated by *Sox17*, only *Efnb2* was shared between the endodermal and endothelial *Sox17* regulons. The marked diversity of *Sox17* regulons as assessed by gene ontology (GO) terms is consistent with SOX17 driving largely different molecular functions in these 2 populations. Indeed, GO-term enrichment patterns suggest that *Sox17* works in endothelial cells to regulate blood-vessel morphogenesis,

cell migration, and sprouting during vasculo-angiogenesis, whereas in endoderm it is more geared toward regulating chemotaxis and signaling pathways such as growth-factor stimulus, serine/threonine kinase and Wnt signaling (Fig. 7B).

### Discussion

Our robust 2-color lineage-tracing strategy, scRNASeq, and use of several computational methods have further characterized *Sox17*-expressing cell populations and expanded our understanding of putative *Sox17* functions during early stages of lineage diversification and tissue specification. Our results not only integrate previous knowledge of *Sox17*-expressing cells but also putatively reveal distinct regulons operating during endothelial and endodermal differentiation, which suggest multiple future lines of investigation.

### Tracing *Sox17*-Expressing Lineages Effectively Captures Early-Stage Vasculo-Angiogenesis and Endothelium-Derived Hematopoiesis

Previous attempts to profile single-cell transcriptomes of the endothelium and hematopoietic system used an antibody panel against multiple cell-surface markers.<sup>19,85</sup> Using just 2 endogenously expressed fluorescent alleles that report short- or long-term expression of *Sox17*, we effectively recorded transcriptomic changes during vasculo-angiogenesis and endothelial-to-hematopoietic transition.

Notably, our findings further delineate some controversial and complex concepts in endothelial and hematopoietic development. We captured a classical hemangioblast population (*Etv2* and *Tal1* positive) that, through our trajectory analysis, gives rise to 2 distinct subtypes of ECs, one of which can advance to become the canonical hemogenic endothelium, supporting the model of *in vivo* unipotency of hemangioblasts.<sup>86</sup> Furthermore, we identified a hemangioblast-like endothelial population (EC3—negative

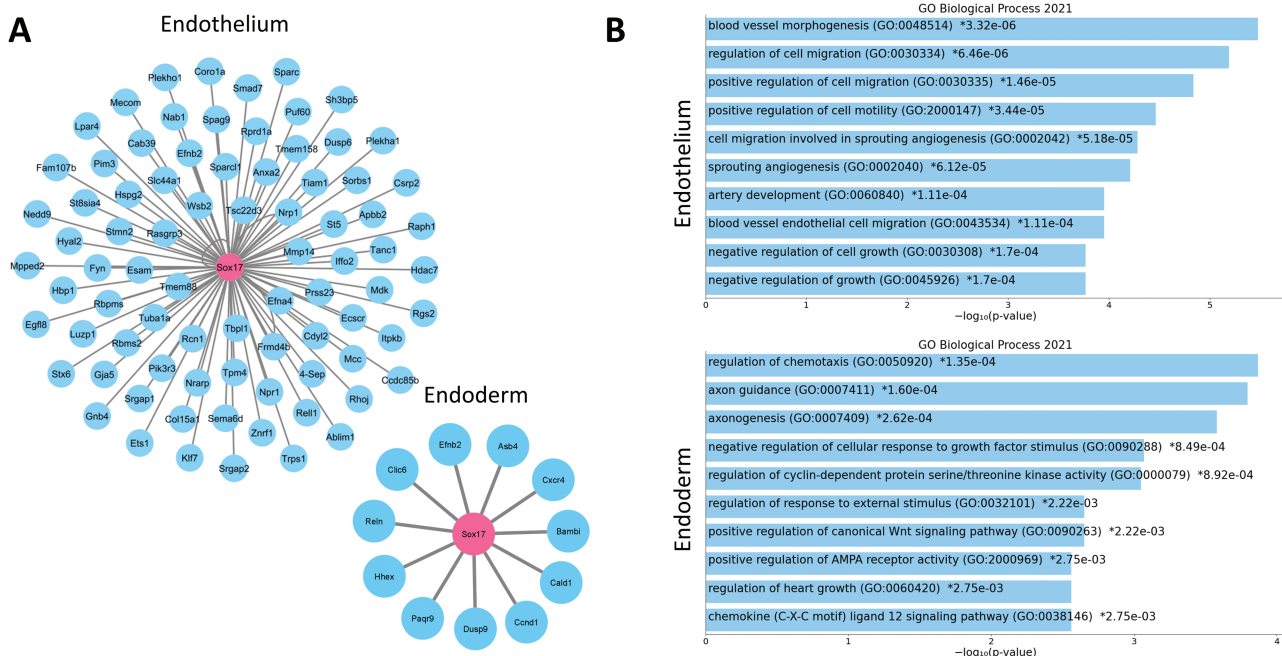


**Figure 7.** Predicted *Sox17*-regulons in endoderm and endothelial cells. (A) pySCENIC predictions of *Sox17* (pink) downstream targets (blue) in the endothelium and endoderm. (B) Gene ontology enrichment analysis of *Sox17* target genes in the endothelium and endoderm.

for *Etv2* and *Tal1*), that expresses many genes suggestive of an extra-embryonic origin and appears to differentiate directly to both erythroids and ECs. Based on recent live imaging<sup>87</sup> and the fact that yolk sacs were omitted from our scRNAseq, we propose that these bipotent progenitors arise in the yolk sac, migrate to the embryo proper, and contribute to both intra-embryonic vascular (potentially at the dorsal aorta, head vasculature, and endocardium—known secondary hematopoiesis sites in the developing embryo) and hematopoietic system likely through *Hox*-dependent mechanisms.

Our analyses of the endothelium raise several areas for further investigation. First, 2 types of ECs seem to arise from hemangioblasts, which differ mostly by expression of *Histone H1* and other cell-cycle genes, but only one can become hemogenic. Based on the known importance of linker histone H1 in cell-fate determination,<sup>88</sup> and of cell-cycle regulation association with endothelial-to-hematopoietic transition,<sup>89</sup> we hypothesize an active participation of *histone H1* during HE specification. Second, whether *Ybx1* and *Tfdp1* regulons, emerging on top of the important endothelial GRN, are critical for endothelial homeostasis or other molecular functions such as migration and morphology, is not known. Lastly, functions of several regulons identified specifically for HE emergence remain to be explored such as *Sox2*, *Sox21*, *Foxn3*, and *Foxf1*.

Although *Sox17* is early and widely expressed within the emerging vasculature system (reflected in our usage of *Sox17<sup>GFP<sup>Cre</sup></sup>* allele), its regulon did not appear among the top 10% most “important” ones in our GRN analysis, indicating moderate, redundant (to other *SoxF* members), or ambiguous functions of *Sox17* in primitive endothelial cells. These results are consistent with *Sox17* having limited functions in the adult endothelial system despite being widely expressed. Indeed, mutations of *Sox17* in the adult vasculature are reported to affect vascular integrity only under challenging conditions such as hypertensive stress.<sup>90-92</sup>

### Transcriptomic Insights Into Hepato-Pancreato-Biliary Development

Unsupervised clustering of the *Sox17-Prox1* endoderm dataset showed 3 distinct clusters of the HPB system, allowing identification of new markers and understudied genes as plausible determinants for each progenitor type. *Ociad2*, encoding a mitochondria-associated protein and top pancreatic marker was recently reported as specifically upregulated in  $\beta$ - rather than  $\alpha$ -cell differentiation from endocrine progenitors,<sup>69</sup> suggesting links between mitochondrial metabolism and insulin-secreting fate acquisition. Similarly, *App* (amyloid precursor protein), expressed in adult pancreatic islets,<sup>93</sup> could influence pancreatic specification from the posterior foregut through autocrine/paracrine signaling. *S100* (Ca<sup>2+</sup>-binding protein with EF-hand motif) family members are also prominent in pancreatic compared to liver and biliary buds, consistent with our previous work showing high *S100a11* in endocrine progenitors and *S100a10* in early *Sox17<sup>+</sup>* endoderm.<sup>94</sup> *S100* functions in cell proliferation, migration, and other signaling pathways are implicated in many cell types,<sup>70</sup> but knowledge of their function during pancreatic development is poor. *Flrt3* (fibronectin leucine-rich transmembrane protein), which contributes to cell adhesion and receptor signaling in other contexts, is present in biliary progenitors,<sup>20</sup> yielding a promising candidate not-yet-determined cellular interactions in biliary development.

Previous attempts to profile single-cell transcriptomes of the developing HPB, perhaps due to technical challenges in obtaining adequate cell numbers, could not resolve all 3 cell types of the system, such as liver-biliary using *FoxA2<sup>eGFP</sup>*, dorsal and ventral pancreas using *Pdx1<sup>GFP</sup>*, and liver-pancreatobiliary using *Prox1<sup>eGFP</sup>* mice. Our *Sox17*-centric strategy complements other datasets (especially *Prox1<sup>eGFP</sup>* as described above), enabling all 3 populations to be distinguished and, further, identification of a subset of liver progenitors with low-hepatic but medium-pancreatobiliary profile, and 3 subsets of biliary progenitors with high-pancreatic, high-biliary, or medium-pancreatobiliary features. These findings indicate the presence of multi- and bipotent progenitors during the gradual segregation of progenitors of the 3 anlagen. These early-stage progenitor cells, besides sharing a high expression of *Sox17* and *Flrt3* with the biliary-committed cells, also express *Phlda2*, a cell-surface Pleckstrin homology-like domain family A member, with potential utility in future cell-sorting analyses. Notably, *Phlda2* is expressed in the ventral gut tube, suggesting a functional association with HPB development, perhaps by regulating epithelial-to-mesenchymal transition via PI3K/AKT during diversification from the posterior foregut.

We also identified several yet-to-be characterized endoderm-active GRNs linked to HPB development including regulons for *Nhlh1* (Nescent Helix-Loop-Helix 1) and *Npdc1* (Neural Proliferation, Differentiation And Control 1), 2 neurogenesis TFs expressed in pancreatic islets and that parallel studies of the human endocrine lineage.<sup>95,96</sup> Our results also unveiled previously unknown but plausibly stochastic functions of the highly redundant *Foxa* TF members,<sup>97</sup> with the *Foxa1* regulon operating in early pancreatic progenitors, the *Foxa2* regulon biased toward mature pancreatic endocrine cells, and the *Foxa3* regulon predominantly active in the hepatic bud.

### Different *Sox17* Regulons in Endoderm and Endothelium

To potentially distinguish *Sox17* functions in the endoderm and endothelium, we compared the pySCENIC-predicted *Sox17*-regulons from the endothelial subset with those derived from the *Sox17-Prox1* endoderm dataset. Of 81 target genes in endothelium compared to 11 predicted in endoderm, *Efnb2* is the only common imputed downstream *Sox17* target. *Efnb2* (an ephrin family member) together with related receptor tyrosine kinases modulates cell-cell communication have well-established roles in arterial/venous specification of endothelial cells, consistent with *Sox17* being indispensable for arterial fate acquisition.<sup>36</sup> *Efnb2* was recently proposed as important in defining the dorsal-ventral axis of foregut,<sup>98</sup> suggesting an unappreciated role of *Sox17* in the endodermal gut tube.

Most other endothelial *Sox17* targets are unsurprisingly related to vascular formation, including tube morphogenesis, tip and stalk cell migration, and motility. In contrast to promoting “proactive” endothelial-cell behavior in response to the surrounding environmental cues, in endodermal cells, *Sox17* may cause more “passive” responses related to sensing chemotactic, growth factor, and particularly Wnt signals. These predicted functions of *Sox17* target genes in endoderm are in agreement with previous studies<sup>99,100</sup> and reinforce the importance of coordinated movements of endodermal cells in response to mesodermal chemotactic cues during gastrulation. Furthermore, the marked difference between endoderm

and endothelial *Sox17*-regulons emphasizes the importance of cellular context in unmasking SOX17 target-gene binding sites, suggesting that SOX17 employs the same strategy seen for other *Sox* family members—to engage in differential protein partnerships so as to economically diversify differentiation programs.<sup>101</sup>

### Identification of *Sox17* in Rare Neural Progenitor Cells

In addition to capturing cells from endodermal, hematopoietic, and endothelial lineages, all are well-established *Sox17*-associated lineages, several neural progenitor cells expressing the canonical markers *Sox1/2/3* and *Nkx6.1* were identified possibly indicating *Sox17* function in these lineages. While *Sox17* function is documented in oligodendrocyte development,<sup>10</sup> little is known about its expression or function in neural progenitors. *SoxF* is associated with neurogenesis in fruit flies<sup>102</sup> and zebrafish,<sup>103</sup> perhaps supporting *Sox17* having a similar role in mammals. In this regard, it is noteworthy that among the low-RNA-content cells excluded from our GFP dataset (Supplementary Methods), a collection of mesenchymal and neural crest-like genes such as *Vim*, *Mest*, *Nes*, *Twist1*, *Prrx2* are expressed. In any case, further analyses and validations are necessary to determine the function of *Sox17* in neural lineages.

### Conclusion

Our analyses of *Sox17*-expressing lineages using scRNAseq consolidate prior knowledge of *Sox17* and provide new insights into the transcriptomic features, GRNs, and developmental trajectories of both hepato-pancreato-biliary and hemato-endothelial systems.

### Acknowledgments

This research was supported by funding provided by Vanderbilt University. We thank the staff of the Vanderbilt Flow Cytometry Shared Resource (FCSR) and the Vanderbilt Cell Imaging Shared Resource (CISR) for their expert assistance. FCSR is supported by CA068485 and DK058404, and CISR by CA68485, DK20593, DK58404, DK59637, and EY08126.

### Conflict of Interest

The authors declared no potential conflicts of interest.

### Author Contributions

L.T.T.: conception and design, collection and assembly of data, data analysis and interpretation, manuscript writing. A.B.O.: conception and design, data analysis, and interpretation. B.L.: collection of data. S.S.: data analysis and interpretation. J-P.C.: data analysis and interpretation. C.V.E.W.: manuscript writing. M.A.M.: conception and design, data analysis and interpretation, financial support, manuscript writing.

### Data Availability

Raw scRNAseq data is at ArrayExpress (E-MTAB-12719), Seurat objects are at <https://zenodo.org/record/7725887#>.

[ZA5jRR\\_MLkI](https://github.com/markmagnuson/2023-Linh-scRNASeq-Mouse-Sox17-Expressing-Lineages). Scripts used to perform quality control, clustering, differential gene expression analysis, Monocle3 and RNAvelocity analyses are at <https://github.com/markmagnuson/2023-Linh-scRNASeq-Mouse-Sox17-Expressing-Lineages>.

### Supplementary Material

Supplementary material is available at *Stem Cells* online.

### References

- Sarkar A, Hochedlinger K. The sox family of transcription factors: versatile regulators of stem and progenitor cell fate. *Cell Stem Cell*. 2013;12(1):15-30. <https://doi.org/10.1016/j.stem.2012.12.007>.
- Kamachi Y, Kondoh H. Sox proteins: regulators of cell fate specification and differentiation. *Development*. 2013;140(20):4129-4144. <https://doi.org/10.1242/dev.091793>.
- She ZY, Yang WX. SOX family transcription factors involved in diverse cellular events during development. *Eur J Cell Biol*. 2015;94(12):547-563. <https://doi.org/10.1016/j.ejcb.2015.08.002>.
- Bowles J, Schepers G, Koopman P. Phylogeny of the SOX family of developmental transcription factors based on sequence and structural indicators. *Dev Biol*. 2000;227(2):239-255. <https://doi.org/10.1006/dbio.2000.9883>.
- Palasingam P, Jauch R, Ng CK, Kolatkar PR. The structure of Sox17 bound to DNA reveals a conserved bending topology but selective protein interaction platforms. *J Mol Biol*. 2009;388(3):619-630. <https://doi.org/10.1016/j.jmb.2009.03.055>.
- Aksoy I, Jauch R, Chen J, et al. Oct4 switches partnering from Sox2 to Sox17 to reinterpret the enhancer code and specify endoderm. *EMBO J*. 2013;32(7):938-953. <https://doi.org/10.1038/emboj.2013.31>.
- Chaves-Moreira D, Mitchell MA, Arruza C, et al. The transcription factor PAX8 promotes angiogenesis in ovarian cancer through interaction with SOX17. *Sci Signal*. 2022;15(728):eabm2496.
- Sinner D, Rankin S, Lee M, Zorn AM. Sox17 and beta-catenin cooperate to regulate the transcription of endodermal genes. *Development*. 2004;131(13):3069-3080. <https://doi.org/10.1242/dev.01176>.
- Kanai-Azuma M, Kanai Y, Gad JM, et al. Depletion of definitive gut endoderm in Sox17-null mutant mice. *Development*. 2002;129(10):2367-2379. <https://doi.org/10.1242/dev.129.10.2367>.
- Sohn J, Natale J, Chew LJ, et al. Identification of Sox17 as a transcription factor that regulates oligodendrocyte development. *J Neurosci*. 2006;26(38):9722-9735. <https://doi.org/10.1523/JNEUROSCI.1716-06.2006>.
- Kim I, Saunders TL, Morrison SJ. Sox17 dependence distinguishes the transcriptional regulation of fetal from adult hematopoietic stem cells. *Cell*. 2007;130(3):470-483. <https://doi.org/10.1016/j.cell.2007.06.011>.
- Pfister S, Jones VJ, Power M, et al. Sox17-dependent gene expression and early heart and gut development in Sox17-deficient mouse embryos. *Int J Dev Biol*. 2011;55(1):45-58. <https://doi.org/10.1387/ijdb.103158sp>.
- Seguin CA, Draper JS, Nagy A, Rossant J. Establishment of endoderm progenitors by SOX transcription factor expression in human embryonic stem cells. *Cell Stem Cell*. 2008;3(2):182-195. <https://doi.org/10.1016/j.stem.2008.06.018>.
- Niakan KK, Ji H, Maehr R, et al. Sox17 promotes differentiation in mouse embryonic stem cells by directly regulating extraembryonic gene expression and indirectly antagonizing self-renewal. *Genes Dev*. 2010;24(3):312-326. <https://doi.org/10.1101/gad.1833510>.
- Qu XB, Pan J, Zhang C, Huang SY. Sox17 facilitates the differentiation of mouse embryonic stem cells into primitive and definitive endoderm in vitro. *Dev Growth Differ*. 2008;50(7):585-593. <https://doi.org/10.1111/j.1440-169x.2008.01056.x>.

16. Han L, Chaturvedi P, Kishimoto K, et al. Single cell transcriptomics identifies a signaling network coordinating endoderm and mesoderm diversification during foregut organogenesis. *Nat Commun.* 2020;11(1):4158. <https://doi.org/10.1038/s41467-020-17968-x>.
17. Nowotschin S, Setty M, Kuo YY, et al. The emergent landscape of the mouse gut endoderm at single-cell resolution. *Nature.* 2019;569(7756):361-367. <https://doi.org/10.1038/s41586-019-1127-1>.
18. Zeng Y, He J, Bai Z, et al. Tracing the first hematopoietic stem cell generation in human embryo by single-cell RNA sequencing. *Cell Res.* 2019;29(11):881-894. <https://doi.org/10.1038/s41422-019-0228-6>.
19. Hou S, Li Z, Zheng X, et al. Embryonic endothelial evolution towards first hematopoietic stem cells revealed by single-cell transcriptomic and functional analyses. *Cell Res.* 2020;30(5):376-392. <https://doi.org/10.1038/s41422-020-0300-2>.
20. Willnow D, Benary U, Margineanu A, et al. Quantitative lineage analysis identifies a hepato-pancreato-biliary progenitor niche. *Nature.* 2021;597(7874):87-91. <https://doi.org/10.1038/s41586-021-03844-1>.
21. Van de Sande B, Flerin C, Davie K, et al. A scalable SCENIC workflow for single-cell gene regulatory network analysis. *Nat Protoc.* 2020;15(7):2247-2276. <https://doi.org/10.1038/s41596-020-0336-2>.
22. Choi E, Kraus MR, Lemaire LA, et al. Dual lineage-specific expression of Sox17 during mouse embryogenesis. *Stem Cells.* 2012;30(10):2297-2308. <https://doi.org/10.1002/stem.1192>.
23. Hao Y, Hao S, Andersen-Nissen E, et al. Integrated analysis of multimodal single-cell data. *Cell.* 2021;184(13):3573-3587.e29. <https://doi.org/10.1016/j.cell.2021.04.048>.
24. McGinnis CS, Murrow LM, Gartner ZJ. DoubletFinder: doublet detection in single-cell RNA sequencing data using artificial nearest neighbors. *Cell Syst.* 2019;8(4):329-337.e4. <https://doi.org/10.1016/j.cels.2019.03.003>.
25. Cao J, Spielmann M, Qiu X, et al. The single-cell transcriptional landscape of mammalian organogenesis. *Nature.* 2019;566(7745):496-502. <https://doi.org/10.1038/s41586-019-0969-x>.
26. Bergen V, Lange M, Peidli S, Wolf FA, Theis FJ. Generalizing RNA velocity to transient cell states through dynamical modeling. *Nat Biotechnol.* 2020;38(12):1408-1414. <https://doi.org/10.1038/s41587-020-0591-3>.
27. Shannon P, Markiel A, Ozier O, et al. Cytoscape: a software environment for integrated models of biomolecular interaction networks. *Genome Res.* 2003;13(11):2498-2504. <https://doi.org/10.1101/gr.1239303>.
28. Gu Z, Eils R, Schlesner M. Complex heatmaps reveal patterns and correlations in multidimensional genomic data. *Bioinformatics.* 2016;32(18):2847-2849. <https://doi.org/10.1093/bioinformatics/btw313>.
29. Argiropoulos B, Humphries RK. Hox genes in hematopoiesis and leukemogenesis. *Oncogene.* 2007;26(47):6766-6776. <https://doi.org/10.1038/sj.onc.1210760>.
30. Cocchia M, Huber R, Pantano S, et al. PLAC1, an Xq26 gene with placenta-specific expression. *Genomics.* 2000;68(3):305-312. <https://doi.org/10.1006/geno.2000.6302>.
31. Lestari B, Naito S, Endo A, et al. Placental mammals acquired functional sequences in NRK for regulating the CK2-PTEN-AKT pathway and placental cell proliferation. *Mol Biol Evol.* 2022;39(2):msab371. <https://doi.org/10.1093/molbev/masab371>
32. Whitfield ML, Sherlock G, Saldanha AJ, et al. Identification of genes periodically expressed in the human cell cycle and their expression in tumors. *Mol Biol Cell.* 2002;13(6):1977-2000. <https://doi.org/10.1091/mbc.02-02-0030>.
33. Trapnell C, Cacchiarelli D, Grimsby J, et al. The dynamics and regulators of cell fate decisions are revealed by pseudotemporal ordering of single cells. *Nat Biotechnol.* 2014;32(4):381-386. <https://doi.org/10.1038/nbt.2859>.
34. La Manno G, Soldatov R, Zeisel A, et al. RNA velocity of single cells. *Nature.* 2018;560(7719):494-498. <https://doi.org/10.1038/s41586-018-0414-6>.
35. Fang JS, Coon BG, Gillis N, et al. Shear-induced Notch-Cx37-p27 axis arrests endothelial cell cycle to enable arterial specification. *Nat Commun.* 2017;8(1):2149. <https://doi.org/10.1038/s41467-017-01742-7>.
36. Corada M, Orsenigo F, Morini MF, et al. Sox17 is indispensable for acquisition and maintenance of arterial identity. *Nat Commun.* 2013;4:2609. <https://doi.org/10.1038/ncomms3609>.
37. Shin D, Garcia-Cardena G, Hayashi S, et al. Expression of ephrinB2 identifies a stable genetic difference between arterial and venous vascular smooth muscle as well as endothelial cells, and marks subsets of microvessels at sites of adult neovascularization. *Dev Biol.* 2001;230(2):139-150. <https://doi.org/10.1006/dbio.2000.9957>.
38. Duan Y, Wang H, Mitchell-Silbaugh K, et al. Heat shock protein 60 regulates yolk sac erythropoiesis in mice. *Cell Death Dis.* 2019;10(10):766.
39. Grisendi S, Bernardi R, Rossi M, et al. Role of nucleophosmin in embryonic development and tumorigenesis. *Nature.* 2005;437(7055):147-153. <https://doi.org/10.1038/nature03915>.
40. Mahotka C, Bhatia S, Kollet J, Grinstein E. Nucleolin promotes execution of the hematopoietic stem cell gene expression program. *Leukemia.* 2018;32(8):1865-1868. <https://doi.org/10.1038/s41375-018-0090-4>.
41. Jariyapong P, Pudgerd A, Cheloh N, et al. Hematopoietic tissue of *Macrobrachium rosenbergii* plays dual roles as a source of hemocyte hematopoiesis and as a defensive mechanism against *Macrobrachium rosenbergii* nodavirus infection. *Fish Shellfish Immunol.* 2019;86:756-763. <https://doi.org/10.1016/j.fsi.2018.12.021>.
42. Kang Y, Kim YW, Yun J, Shin J, Kim A. KLF1 stabilizes GATA-1 and TAL1 occupancy in the human beta-globin locus. *Biochim Biophys Acta.* 2015;1849(3):282-289.
43. Tallack MR, Whittington T, Yuen WS, et al. A global role for KLF1 in erythropoiesis revealed by ChIP-seq in primary erythroid cells. *Genome Res.* 2010;20(8):1052-1063. <https://doi.org/10.1101/gr.106575.110>.
44. Liu F, Li D, Yu YY, et al. Induction of hematopoietic and endothelial cell program orchestrated by ETS transcription factor ER71/ETV2. *EMBO Rep.* 2015;16(5):654-669. <https://doi.org/10.15252/embr.201439939>.
45. Koyano-Nakagawa N, Garry DJ. ETV2 as an essential regulator of mesodermal lineage development. *Cardiovasc Res.* 2017;113(11):1294-1306. <https://doi.org/10.1093/cvr/cvx133>.
46. Casie Chetty S, Sumanas S. Ets1 functions partially redundantly with ETV2 to promote embryonic vasculogenesis and angiogenesis in zebrafish. *Dev Biol.* 2020;465(1):11-22. <https://doi.org/10.1016/j.ydbio.2020.06.007>.
47. Park JI, Kim KS, Kong SY, Park KS. Novel function of E26 transformation-specific domain-containing protein ELK3 in lymphatic endothelial cells. *Oncol Lett.* 2018;15(1):55-60.
48. Francois M, Caprini A, Hosking B, et al. Sox18 induces development of the lymphatic vasculature in mice. *Nature.* 2008;456(7222):643-647. <https://doi.org/10.1038/nature07391>.
49. Heo SH, Cho JY. ELK3 suppresses angiogenesis by inhibiting the transcriptional activity of ETS-1 on MT1-MMP. *Int J Biol Sci.* 2014;10(4):438-447. <https://doi.org/10.7150/ijbs.8095>.
50. Tsuji-Tamura K, Morino-Koga S, Suzuki S, Ogawa M. The canonical smooth muscle cell marker TAGLN is present in endothelial cells and is involved in angiogenesis. *J Cell Sci.* 2021;134(15):jcs254920. <https://doi.org/10.1232/jcs.254920>
51. Gopal SK, Greening DW, Mathias RA, et al. YBX1/YB-1 induces partial EMT and tumorigenicity through secretion of angiogenic factors into the extracellular microenvironment. *Oncotarget.* 2015;6(15):13718-13730. <https://doi.org/10.18632/oncotarget.3764>.
52. Eliseeva IA, Kim ER, Guryanov SG, Ovchinnikov LP, Lyabin DN. Y-box-binding protein 1 (YB-1) and its functions. *Biochemistry (Mosc).* 2011;76(13):1402-1433. <https://doi.org/10.1134/S0006297911130049>.

53. Zhan W, Wang W, Han T, et al. COMMD9 promotes TFDP1/E2F1 transcriptional activity via interaction with TFDP1 in non-small cell lung cancer. *Cell Signal*. 2017;30:59-66. <https://doi.org/10.1016/j.cellsig.2016.11.016>.
54. Morimoto Y, Mizushima T, Wu X, et al. miR-4711-5p regulates cancer stemness and cell cycle progression via KLF5, MDM2 and TFDP1 in colon cancer cells. *Br J Cancer*. 2020;122(7):1037-1049. <https://doi.org/10.1038/s41416-020-0758-1>.
55. Wang W, Wang HJ, Wang B, et al. The role of the Y box binding protein 1 C-terminal domain in vascular endothelial cell proliferation, apoptosis, and angiogenesis. *DNA Cell Biol*. 2016;35(1):24-32. <https://doi.org/10.1089/dna.2015.2908>.
56. Pham TP, Bink DI, Stanicek L, et al. Long non-coding RNA Aeric controls DNA damage repair via YBX1 to maintain endothelial cell function. *Front Cell Dev Biol*. 2020;8:619079. <https://doi.org/10.3389/fcell.2020.619079>.
57. Gao L, Tober J, Gao P, et al. RUNX1 and the endothelial origin of blood. *Exp Hematol*. 2018;68:2-9. <https://doi.org/10.1016/j.exphem.2018.10.009>.
58. Dou DR, Calvanese V, Sierra MI, et al. Medial HOXA genes demarcate haematopoietic stem cell fate during human development. *Nat Cell Biol*. 2016;18(6):595-606. <https://doi.org/10.1038/ncb3354>.
59. Zaidan N, Nitsche L, Diamanti E, et al. Endothelial-specific Gata3 expression is required for hematopoietic stem cell generation. *Stem Cell Rep*. 2022;17(8):1788-1798. <https://doi.org/10.1016/j.stemcr.2022.06.008>.
60. Philip Creamer J, Luff SA, Yu H, Sturgeon CM. CD1d expression demarcates CDX4+ hemogenic mesoderm with definitive hematopoietic potential. *Stem Cell Res*. 2022;62:102808. <https://doi.org/10.1016/j.scr.2022.102808>.
61. Azzoni E, Frontera V, Anselmi G, et al. The onset of circulation triggers a metabolic switch required for endothelial to hematopoietic transition. *Cell Rep*. 2021;37(11):110103.
62. Jung HS, Uenishi G, Park MA, et al. SOX17 integrates HOXA and arterial programs in hemogenic endothelium to drive definitive lympho-myeloid hematopoiesis. *Cell Rep*. 2021;34(7):108758. <https://doi.org/10.1016/j.celrep.2021.108758>.
63. Lilly AJ, Costa G, Largeot A, et al. Interplay between SOX7 and RUNX1 regulates hemogenic endothelial fate in the yolk sac. *Development*. 2016;143(23):4341-4351.
64. Yi Z, Cohen-Barak O, Hagiwara N, et al. Sox6 directly silences epsilon globin expression in definitive erythropoiesis. *PLoS Genet*. 2006;2(2):e14. <https://doi.org/10.1371/journal.pgen.0020014>.
65. Sturtzel C, Lipnik K, Hofer-Warbinek R, et al. FOXF1 mediates endothelial progenitor functions and regulates vascular sprouting. *Front Bioeng Biotechnol*. 2018;6:76. <https://doi.org/10.3389/fbioe.2018.00076>.
66. Schnerch A, Lee JB, Graham M, Guezguez B, Bhatia M. Human embryonic stem cell-derived hematopoietic cells maintain core epigenetic machinery of the polycomb group/trithorax group complexes distinctly from functional adult hematopoietic stem cells. *Stem Cells Dev*. 2013;22(1):73-89. <https://doi.org/10.1089/scd.2012.0204>.
67. Hou J, Wei W, Saund RS, et al. A regulatory network controls nephrocan expression and midgut patterning. *Development*. 2014;141(19):3772-3781. <https://doi.org/10.1242/dev.108274>.
68. Rodriguez-Seguel E, Mah N, Naumann H, et al. Mutually exclusive signaling signatures define the hepatic and pancreatic progenitor cell lineage divergence. *Genes Dev*. 2013;27(17):1932-1946. <https://doi.org/10.1101/gad.220244.113>.
69. Scavuzzo MA, Hill MC, Chmielowiec J, et al. Endocrine lineage biases arise in temporally distinct endocrine progenitors during pancreatic morphogenesis. *Nat Commun*. 2018;9(1):3356. <https://doi.org/10.1038/s41467-018-05740-1>.
70. Wu Y, Zhou Q, Guo F, et al. S100 proteins in pancreatic cancer: current knowledge and future perspectives. *Front Oncol*. 2021;11:711180. <https://doi.org/10.3389/fonc.2021.711180>.
71. Hansel DE, Rahman A, Wehner S, et al. Increased expression and processing of the Alzheimer amyloid precursor protein in pancreatic cancer may influence cellular proliferation. *Cancer Res*. 2003;63(21):7032-7037.
72. Wilson ME, Yang KY, Kalousova A, et al. The HMG box transcription factor Sox4 contributes to the development of the endocrine pancreas. *Diabetes*. 2005;54(12):3402-3409. <https://doi.org/10.2337/diabetes.54.12.3402>.
73. Lotto J, Drissler S, Cullum R, et al. Single-cell transcriptomics reveals early emergence of liver parenchymal and non-parenchymal cell lineages. *Cell*. 2020;183(3):702-716.e14. <https://doi.org/10.1016/j.cell.2020.09.012>.
74. Mu T, Xu L, Zhong Y, et al. Embryonic liver developmental trajectory revealed by single-cell RNA sequencing in the Foxa2(eGFP) mouse. *Commun Biol*. 2020;3(1):642. <https://doi.org/10.1038/s42003-020-01364-8>.
75. Winters SJ, Scoggins CR, Appiah D, Ghooray DT. The hepatic lipidome and HNF4alpha and SHBG expression in human liver. *Endocr Connect*. 2020;9(10):1009-1018. <https://doi.org/10.1530/EC-20-0401>.
76. Yu Y, Jiang L, Wang H, et al. Hepatic transferrin plays a role in systemic iron homeostasis and liver ferroptosis. *Blood*. 2020;136(6):726-739. <https://doi.org/10.1182/blood.2019002907>.
77. Merkel M, Weinstock PH, Chajek-Shaul T, et al. Lipoprotein lipase expression exclusively in liver: a mouse model for metabolism in the neonatal period and during cachexia. *J Clin Invest*. 1998;102(5):893-901. <https://doi.org/10.1172/JCI2912>.
78. Han S, Tan C, Ding J, et al. Endothelial cells instruct liver specification of embryonic stem cell-derived endoderm through endothelial VEGFR2 signaling and endoderm epigenetic modifications. *Stem Cell Res*. 2018;30:163-170. <https://doi.org/10.1016/j.scr.2018.06.004>.
79. Spence JR, Lange AW, Lin SC, et al. Sox17 regulates organ lineage segregation of ventral foregut progenitor cells. *Dev Cell*. 2009;17(1):62-74. <https://doi.org/10.1016/j.devcel.2009.05.012>.
80. Hou J, Charters AM, Lee SC, et al. A systematic screen for genes expressed in definitive endoderm by Serial Analysis of Gene Expression (SAGE). *BMC Dev Biol*. 2007;7:92. <https://doi.org/10.1186/1471-213X-7-92>.
81. Bohuslavova R, Smolik O, Malfatti J, et al. NEUROD1 is required for the early alpha and beta endocrine differentiation in the pancreas. *Int J Mol Sci*. 2021;22(13):6713. <https://doi.org/10.3390/ijms22136713>.
82. Duvall E, Benitez CM, Tellez K, et al. Single-cell transcriptome and accessible chromatin dynamics during endocrine pancreas development. *Proc Natl Acad Sci USA*. 2022;119(26):e2201267119.
83. Nissim S, Weeks O, Talbot JC, et al. Iterative use of nuclear receptor Nr5a2 regulates multiple stages of liver and pancreas development. *Dev Biol*. 2016;418(1):108-123. <https://doi.org/10.1016/j.ydbio.2016.07.019>.
84. Tachmatzidi EC, Galanopoulou O, Talianidis I. Transcription control of liver development. *Cells*. 2021;10(8):2026. <https://doi.org/10.3390/cells10082026>.
85. Zhu Q, Gao P, Tober J, et al. Developmental trajectory of prehematopoietic stem cell formation from endothelium. *Blood*. 2020;136(7):845-856. <https://doi.org/10.1182/blood.2020004801>.
86. Lancrin C, Sroczynska P, Stephenson C, et al. The haemangioblast generates haematopoietic cells through a haemogenic endothelium stage. *Nature*. 2009;457(7231):892-895. <https://doi.org/10.1038/nature07679>.
87. Collart C, Ciccarelli A, Ivanovitch K, et al. The migratory pathways of the cells that form the endocardium, dorsal aortae, and head vasculature in the mouse embryo. *BMC Dev Biol*. 2021;21(1):8. <https://doi.org/10.1186/s12861-021-00239-3>.
88. Sollberger G, Streeck R, Apel F, et al. Linker histone H1.2 and H1.4 affect the neutrophil lineage determination. *Elife*. 2020;9:e52563. <https://doi.org/10.7554/elife.52563>.
89. Canu G, Athanasiadis E, Grandy RA, et al. Analysis of endothelial-to-hematopoietic transition at the single cell level identifies cell cycle regulation as a driver of differentiation. *Genome Biol*. 2020;21(1):157. <https://doi.org/10.1186/s13059-020-02058-4>.

90. Lee S, Kim IK, Ahn JS, et al. Deficiency of endothelium-specific transcription factor Sox17 induces intracranial aneurysm. *Circulation*. 2015;131(11):995-1005. <https://doi.org/10.1161/CIRCULATIONAHA.114.012568>.
91. Wang TM, Wang SS, Xu YJ, et al. SOX17 loss-of-function mutation underlying familial pulmonary arterial hypertension. *Int Heart J*. 2021;62(3):566-574. <https://doi.org/10.1536/ihj.20-711>.
92. Park CS, Kim SH, Yang HY, et al. Sox17 deficiency promotes pulmonary arterial hypertension via HGF/c-Met signaling. *Circ Res*. 2022;131(10):792-806. <https://doi.org/10.1161/CIRCRESAHA.122.320845>.
93. Kulas JA, Puig KL, Combs CK. Amyloid precursor protein in pancreatic islets. *J Endocrinol*. 2017;235(1):49-67. <https://doi.org/10.1530/JOE-17-0122>.
94. Osipovich AB, Dudek KD, Greenfest-Allen E, et al. A developmental lineage-based gene co-expression network for mouse pancreatic beta-cells reveals a role for Zfp800 in pancreas development. *Development*. 2021;148(6):dev196964. <https://doi.org/10.12422/dev.196964>.
95. Alvarez-Dominguez JR, Donaghey J, Rasouli N, et al. Circadian entrainment triggers maturation of human in vitro islets. *Cell Stem Cell*. 2020;26(1):108-122.e10. <https://doi.org/10.1016/j.stem.2019.11.011>.
96. Shrestha S, Erikson G, Lyon J, et al. Aging compromises human islet beta cell function and identity by decreasing transcription factor activity and inducing ER stress. *Sci Adv*. 2022;8(40):eabo3932.
97. Kaestner KH. The making of the liver: developmental competence in foregut endoderm and induction of the hepatogenic program. *Cell Cycle*. 2005;4(9):1146-1148. <https://doi.org/10.4161/cc.4.9.2033>.
98. Lewis AE, Kuwahara A, Franzosi J, Bush JO. Tracheal separation is driven by NKX2-1-mediated repression of Efnb2 and regulation of endodermal cell sorting. *Cell Rep*. 2022;38(11):110510.
99. Nair S, Schilling TF. Chemokine signaling controls endodermal migration during zebrafish gastrulation. *Science*. 2008;322(5898):89-92. <https://doi.org/10.1126/science.1160038>.
100. Chuai M, Hughes D, Weijer CJ. Collective epithelial and mesenchymal cell migration during gastrulation. *Curr Genomics*. 2012;13(4):267-277. <https://doi.org/10.2174/138920212800793357>.
101. Kamachi Y, Uchikawa M, Kondoh H. Pairing SOX off: with partners in the regulation of embryonic development. *Trends Genet*. 2000;16(4):182-187. [https://doi.org/10.1016/s0168-9525\(99\)01955-1](https://doi.org/10.1016/s0168-9525(99)01955-1).
102. Cremazy F, Berta P, Girard F. Genome-wide analysis of Sox genes in *Drosophila melanogaster*. *Mech Dev*. 2001;109(2):371-375. [https://doi.org/10.1016/s0925-4773\(01\)00529-9](https://doi.org/10.1016/s0925-4773(01)00529-9).
103. Hu Y, Wang B, Du H. A review on sox genes in fish. *Rev Aquacult*. 2021;13(4):1986-2003. <https://doi.org/10.1111/raq.12554>.